Article

Not peer-reviewed version

Hydroxyhydroquinone and quassinoids as promising compounds with hypoglycemic activity through redox balance

Paulo Roberto dos Santos , Sidineia Danetti , Joseph Rastegar , Wellington De Souza , Rafaele Frassini , Fernando Joel Scariot , Sidnei Moura , Mariana Roesch-Ely *

Posted Date: 2 August 2023

doi: 10.20944/preprints202308.0046.v1

Keywords: hydroxyhydroquinone; quassinoids; glycemia

Article

Hydroxyhydroquinone and Quassinoids as Promising Compounds with Hypoglycemic Activity through Redox Balance

Paulo R. dos Santos [1], Sidinéia Danetti [1], A. Joseph Rastegar [3], Wellington V. de Souza [3], Rafaele Frassini [3], Fernando J. Scariot [2], Sidnei Moura [1] and Mariana Roesch-Ely [3,*]

[1] Laboratory of Biotechnology of Natural and Synthetics Products, University of Caxias do Sul, Brazil
[2] Laboratory of Applied Microbiology, University of Caxias do Sul, Brazil
[3] Laboratory of Applied Toxicology and Bioproducts, University of Caxias do Sul, Brazil
* Correspondence: mrely@ucs.br; Tel.: +55-54-3218-2100

Abstract: Reactive oxygen species (ROS) are essential signaling molecules involved in almost all metabolic processes. In the present study, a HepG2 insulin resistant cell model (HepG2/IRM) was chosen to investigate the efficacy of hydroxyhydroquinone (HHQ); quassinoids from *Picrasma crenata* and flavonoids from *Rourea cuspidata* as potential glycemic controlling agents for insulin sensitization. HHQ was synthetized and extracts from *P. crenata* and *R. cuspidata* were tested in hepatic cell line; which were evaluated through cytotoxic activity; levels of ROS; ATP; mitochondrial membrane potential and expression of FoxO1 protein in a high glucose environment. Our results demonstrate that the HHQ, quassinoids and flavonoids were not toxic to cells at concentrations up to 50mM and 50 mg/mL in HepG2/IRM and HepG2. ROS activity was increased for all groups with insulin induction upon glucose consumption. HHQ and quassinoids downregulate the expression of FoxO1 in comparison to cells exposed to flavonoids. The results here presented suggests that quassinoids may act on nuclear glucocorticoid receptors to inhibit FoxO1 expression by competing with cortisol and HHQ can act as ROS scavenger to ameliorate mitochondria activity and modulate ATP generation. This study provides a pharmacological basis for the application of HHQ, quassinoids from *P. crenata* and flavonoids from *R. cuspidata* in the treatment of metabolic diseases such as type 2 diabetes mellitus.

Keywords: hydroxyhydroquinone; quassinoids; glycemia

---

1. Introduction

All living organisms produce reactive oxygen species (ROS) as a result of cellular metabolism. Compartmentalization of ROS production within cells, however, elicit redox signaling or oxidative damage in specific organelles [1]. There are several intracellular compartments that are sources of ROS and present different effects in metabolism [2]. Despite the existence of a variety of ROS origins, mitochondria and NADPH oxidases are listed as major sites of ROS balance [3]. NADPH and mitochondria oxidase processes interact, which contribute to the gradual progression of oxidative stress as suggested by Daiber [4].

ROS are found in mitochondria within most mammalian cells and are therefore highly involved in oxidative stress. Increased production might contribute to mitochondrial damage in a range of pathologies. They also play a significant role in a redox signaling system from the organelle to the rest of the cell that leads to mild uncoupling resulting in an augmented ROS production [1]. Imbalance between energy intake and expenditure drives the mitochondrial dysfunction, characterized by a reduced ratio of energy production (lower ATP concentration) [5]. It is theorized that mitochondria of diabetic cells, when exposed to high glucose and fatty acid concentrations, may lead toward greater oxygen use and higher oxidation potential, thereby forming more ROS. Mitochondrial dysfunction in insulin-sensitive tissues, including muscle, heart, and liver, may also contribute to deterioration in the diabetic state over time [5,6]. However, whether defects in mitochondria are primary or secondary, more investigation is needed. Even if mitochondrial dysfunction were secondary to insulin resistance, mitochondrial defects exacerbate hyperglycemia once the insulin resistance has taken effect and leads to a progressive state of the diabetic condition [6].

To ameliorate hepatic insulin resistance and increase sensitivity, various synthetic pharmaceuticals have been discovered and looking for new pharmacological activities for existing candidates became potential task. Some of these compounds results in drug resistance and shows various side effects in long-term use. Metformin the active compound in *Galeca Officinalis* (Goat's rue) is a good example. Metformin is used as a first-line therapeutic drug to prevent hepatic glucose generation [7].

The identification of additional natural active compounds which can potentially improve hepatic insulin sensitivity with least side effects are mandatory. Hydroxyhydroquinone or 1,2,4-trihydroxy benzene (HHQ) is a simple aromatic molecule with redox potential like flavonoids and its redox properties. Its low redox potential and it oxidate homologous hydroxybenzoquinone makes a good flavonoid analog to test verifying phenolic activities to improve cell insulin sensitivity [8]. According to Kargl et al. (2017) [9], phenolic compound such flavonoids can increase serum cortisol by inhibition of 11β-hydroxysteroid dehydrogenase type 2 enzyme. In this sense, some phenolic compounds present in plants used for the treatment of type II diabetes, such as *Rourea cuspidata*, miraruira, tend to act on 11β-hydroxysteroid dehydrogenase type 1 as enzyme inhibitors to mitigate non-adrenal cortisol production [10]. Resveratrol is an example of active polyphenol known for anti-diabetic effects in both animals and humans. Resveratrol has been shown to be involved in maintaining glucose homeostasis, decreasing insulin resistance, protecting pancreatic β-cells, promoting insulin secretion and relieving metabolic disorders [7].

Quassinoids compound obtained from Brazilian quassia tree (*Picrama crenata*) have been used as antidiabetic phytotherapy. Its activity is not clear, but the major compounds present in quassia stems and barks named quassinoids may be the active compounds, since their structures are similar to steroid molecular skeleton. The quassinoids can acts like glucocorticoid and mineral corticoid and can reduce glycemia by cortisol inhibition on liver and inducing glycosuria [11].

It is known that insulin resistance and gluconeogenesis are complementary biochemical phenomena mediated by FOXO1, a nuclear protein in hepatocytes that acts as a signal for glucose metabolism [12]. Once activated, insulin receptors in the liver modulate the downstream insulin signaling, including the phosphatidylinositol 3-kinase (PI3K) and protein kinase B (PKB/AKT). AKT phosphorylates several substrates such as forkhead box O1 (FOXO1), controlling the transcription of genes encoding gluconeogenic enzymes, and glycogen synthase kinase [13]. In the presence of insulin, hydroxyhydroquinone and quassinoids compounds were able to decrease expression of FOXO1, most likely inhibiting gluconeogenesis and ultimately reducing glucose production.

In the present study a HepG2 insulin resistant cell model was chosen to investigate the efficacy of hydroxyhydroquinone and quassinoids extracts as promising compounds with hypoglycemic activity through redox balance. Hydroxyhydroquinone was synthetized and a series of quassinoids from *P. crenata* and flavonoids from *R. cuspidata* extracts were identified and tested in HepG2 cells, which were evaluated through cytotoxic activity, levels of ROS, ATP, mitochondrial membrane potential (MMP), and FoxO1 expression in a high glucose environment.

2. Materials and Methods

2.1. Synthesis of Hydroxyhydroquinone (HHQ) (Scheme 1)

HHQ was prepared according Humbarger et al. (2018) [14]. On the first step, 30.0 g of 1,4-hydroquinone (HQ) (272 mmol, 1.0 eq) was suspended on 200 mL of ethyl acetate/aqueous H_2SO_4 3% 80/20 v/v with 0.5 g of iodine as catalyst (3.9 mmol, 0.014 eq) on a glass half-liter round bottle flask. The stirred solution was added with 50.0 mL of H_2O_2 30% (489 mmol, 1.8 eq) dropwise to maintain temperature around 45°C by 3 h. After cooling overnight on freezer, brownish yellow crystals of 1,4-benzoquinone (BQ) were filtered out by vacuum, washed with cooled water/methanol and dried in air for 24h. Yield of BQ was 20.55g, approximately 70%.

On the second step, a solution of 43.0 g of acetic anhydride (421 mmol, 2.2 eq), 22.8 g of acetic acid (379 mmol, 2.0 eq) and 4.0 g of H_2SO_4 98 % (41 mmol, 0.2 eq) was previously prepared on a glass half-liter two necks round bottle flask with vigorous stirring. The amount of 20.55 g of BQ (190 mmol, 1.0 eq) was added portion wise in order to maintain the temperature around 45 °C (exothermic reaction). After complete addition of BQ, the reaction was allowed to cool to room temperature and maintain stirring over 30 min when white solids were formed. The reacted moisture was added with 200 mL of ice water, filtered by vacuum and washed with excess of ice water. The white solids were dried on freeze drier for 24h. Yield of 1,2,4-AcBz was 47.3g, ~99%.

On the third step, 47.3g of 1,2,4-AcBz (187 mmol, 1.0 eq) was suspended in 180 mL of methanol, 100 mL of water and 1.55 mL of HCl 37%. The moisture was refluxed for 7 h and maintained at room temperature for 14 h. The solvents were removed by vacuum evaporator and the brownish solids were suspended in 140 mL of hot ethyl acetate. Sodium hydrogen carbonate (14g) and 1.4 g of active charcoal was added under vigorous stirring while the system was refluxed for 30 min. The solids were removed in vacuum filter and the solvent was removed by vacuum evaporator. The HHQ crystallizes as an orange semisolid form, yielding 23.35g (99%). The product was stored under inert atmosphere (N_2) in dark conditions at room temperature.

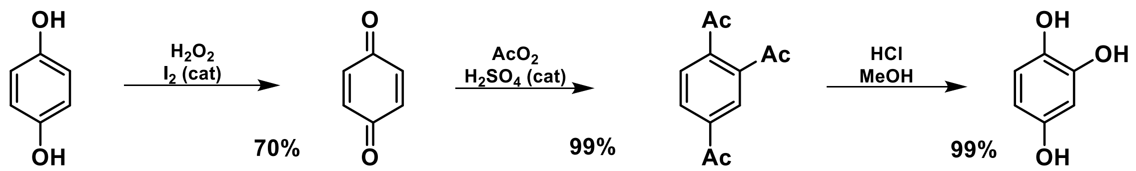

Figure 1. Scheme of synthetic route of HHQ.

2.2. Vegetable material

2.2.1. Extracts of P. crenata

The vegetable material (*P. crenata*) was collected from Marques de Souza City, RS, Brazil (29°14′38″ S 52°11′18″ W). Stem parts without bark were dried over dry oven (7 days) and crushed on Willey® type mill (1 mm mesh). Extracts were prepared according to Cardoso et al. (2009) [15]. When, 10g of powder were extracted with 100 mL of ethanol:water 50:50% v/v at by reflux for 2 h. Solvent was removed on rotavapor.

2.2.2. Chromatographic assay of P. crenata

Chromatographic method was used to determine chemical composition of *P. crenata* extract. It was performed according to Cardoso et al. (2009) [15]. The chromatographic system was composed of UFLC Shimadzu compounded with two pumps LC 20A, degasser DGU 20A, auto injector SIL20A HT, column oven CTO 20A and controller CBM 20A. The separation process was performed with RP 18 column (Agilent Zorbax 250mm x 4.7mm, 5 mm particle size) at 25 °C. Gradient system was composed for water(A) and metanol(B): 0-2 min (90%A:10%B), 2-10 min (60%A:40%B), 10-20 min (50%A: 50%B), 20-25 min (50%A:50%B), 25-30 min (90%A:10%B). Total flow at 1.0 mL min^{-1} and sample volume injection of 20 µL. HRMS detection system was composed by Micro TOF-Q II (Bruker Scientific) with electrospray source (ESI) operated at 200 °C, dry gas flow (N_2) 10 L.min^{-1}, gas capilar pressure 5 bar. Spectrometer configuration: spectral window 50 to 2200 m/z, data record rate: 2 scans.s^{-1}, controlled by Compass Hystar interface software (version 3.2). The runs were recorded in mode positive and negative ions. Data treatments were performed in Compass DataAnalysis 4.3.

2.2.3. Extracts of R. cuspidata

R. cuspidata extracts (Miraruira) were prepared according Laikowski et al. (2017) [10]. The plant material (lianas) was dried in air oven at 45 °C. The powdered material (10g) was extracted in ethanol:H_2O 50:50 (100 mL) by reflux 2 h, the solution was filtered and the solvent was removed by vacuum. Crude solids were resuspended in water and extracted with hexane to remove fatty acids and greasy compounds. The aqueous fraction was dried by vacuum and used in our experiments. Chemical composition was determined by ESI-TOF-MS by direct infusion using same device settings used in 2.2.2.

2.3. Cell culture and cytotoxic assay

The established human HepG2 hepatoma cell line was obtained from the American Type Culture Collection (MD, USA). HepG2 cells were grown in Dulbecco's modified Eagle's medium (DMEM) supplemented with 10% fetal bovine serum (Gibco) under standard cell culture conditions, with humidified atmosphere, 5% CO_2 and 37 °C. Cell viability of HepG2 against different treatment was measured using the MTT assay. Briefly, cells were seeded into the 96-well plates at a density of 8.0 x 10^4 cells/mL. After 24h, cells were treated with different concentrations of extracts and incubated for 24 h. Negative controls were treated with the same amounts of solution for 24 h. The medium was removed and 1 mg/mL MTT dye in serum-free medium was added to the wells. Plates were incubated at 37 °C for 2 h in humidified 5% CO_2 atmosphere. Subsequently, the MTT solution was removed, and the obtained formazan violet product was dissolved in 100 mL DMSO. Absorbance was measured using a microplate reader (Spectra Max M2e, Molecular Devices, USA) at 570 nm. All readings were compared with the control, which represented 100% viability. Each experiment was performed in triplicate and independently repeated at least four times.

2.4. Insulin resistance model (HepG2/IRM) and glucose uptake

HepG2 cell lines have been used as insulin resistance model in several studies. This protocol was adapted from Kheirollahzadeh et al. (2022) [16]. In order to establish an insulin-resistant cell model (HepG2/IRM), a gradient of insulin at different concentrations was initially tested for viability through MTT and further glucose quantification was performed. Therefore, cells were seeded in 96-well plates at 8,0 x 10^4 cells/mL in DMEM supplemented with a high glucose concentration (25 mmol/L). After 24 h incubation, cells were treated with insulin at concentrations of 10^{-4} mol/L to 10^{-7} mol/L. Best parameters for insulin concentration was selected for IR model and further experiments were processed with insulin at 5µM for 24h. At the end of the incubation period, glucose concentrations were determined using the glucose oxidase method through glucometer measurements (Accu-Chek®Guide; Roche). According to the manufacture instructions, glucose dehydrogenase present in the strip converts the glucose in the culture media sample to gluconolactone, generating a reaction that liberates two electrons that react with a coenzyme (PQQ) electron acceptor. Glucose was assayed in 50 µL of the media and the edges of the stripes were immerged in solution for measurement. The percentage of cellular glucose in media was determined as the difference between glucose concentration before and after insulin treatment relative to control non-insulin treated cells. After 24h exposition to insulin at 5µM, cells were treated with the highest non-cytotoxic concentration of diferent extracts for 24h.

2.5. Mitochondria Membrane Potential (MMP) Assay and ROS activity

Mitochondria membrane potential was evaluated using mitochondria membrane potential kit (MAK 159, Sigma-Aldrich). HepG2 and HepG2/IRM cells were plated in 6-well plates at 3,0 x 10^5 cells/mL and exposed to different treatments. After adherence, cells were treated with the highest non-cytotoxic concentration of diferent extracts for 24h. The protocol was modified from manufacture instructions to 6 well plates and 300µL of dye loading solution of JC-10 was diluted in buffer A (1:100) and loaded in each well. After 1h of incubation, 300 µL of loading solution B was added to each well and cells were monitored in microscope with fluorescent filters (Olympus, BX43). JC-10 is a cationic lipophilic dye that generates red-fluorescent aggregates (λex = 540nm / λem = 590nm) in polarized mitochondrial membrane. Failure to retain JC-10 in the mitochondria, leads to a collapse in membrane potential and the dye returns to its monomeric green form (λex = 490nm / λem = 525nm).

Mitochondria activity was also monitored trough incubation of 3,3′-dihexyloxacarbocyanine iodide - DiOC6 stain (318426, Sigma-Aldrich). HepG2 and HepG2/IRM cells were plated in 6-well plates at 3,0 x 10^5 cells/mL and exposed to the highest non-cytotoxic concentration of diferent extracts for 24h. DiO6 at final concentration of 40 nM was incubated in each treated media well during 40 min before analysis in microscope with fluorescent filters (λex = 481nm/ λem = 501nm, Olympus, BX43).

Reactive oxygen species (ROS) activity was processed using 2′,7′-dichlorodihydrofluorescein diacetate (DCFH-DA) (35845, Sigma-Aldrich) protocol in HepG2 and HepG2/IRM in 6-well plates at 3,0 x 10^5 cells/mL and exposed to the highest non-cytotoxic concentration of diferent extracts for 24h. DCPH-DA at final concentration of 10μM was applied in each treated media well and cells were incubated during 40 min before analysis in microscope with fluorescent filters (λex = 485nm/ λem = 530nm, Olympus, BX43).

Mitochondrial membrane potential and reactive oxygen species were measured by flow cytometry. HepG2 and HepG2/IRM cells were plated in 6-well plates at 3,0 x 10^5 cells/mL and exposed to different treatments. After 24h, cells were exposed to the highest non-cytotoxic concentration of diferent extracts for 24h. The negative control groups were treated with the same amount of aqueous solution used for the extracts. The intensity of fluorescence from 10,000 cells were quantified by a BD FACSCalibur four colors flow cytometer (Becton Dickinson LTDA). Data were collected by CellQuest Pro software (BD Biosciences) and analyzed using FlowJo (TreeStar, Inc). Experimental procedures were performed at least in duplicate. Changes in the MMP as a result of mitochondrial depolarization were measured using the method of incorporation of 3,3′-dihexyloxacarbocyanine iodide (DioC6(3); Molecular Probes Inc.,USA) according to Frozza et al. (2017) [17]. Briefly, treated and untreated cells were harvested by trypsin, washed once in PBS, and then stained with DioC6(3) (175 nM) 30 min and analyzed by flow cytometry using FL1 filter (488/533) filter. Measurement of intracellular levels of ROS in cells were stained by 2′,7′-dichlorofluorescein diacetate (DCFH-DA, Sigma) with modifications. DCFH-DA penetrates the intracellular matrix of cells to be oxidized by ROS to fluorescent dichlorofluorescein (DCF). Fluorescent dye solutions (10 uM) was added to the cells and incubated for 30 min at 37 °C in the dark. The levels of ROS were analyzed at an excitation 488 nm and emission 533 nm.

2.6. Adenosine triphosphate (ATP) activity

ATP activity was monitored through the CellTiter-Glo® Luminescent Cell Viability Assay (G7570, Promega, US). This protocol allows determining the number of viable cells in culture based on quantitation of the ATP through the addition of a thermostable luciferase, generating a luminescent signal. Therefore, HepG2 and HepG2/IRM cells were plated in 6-well plates at 3,0 x 10^5 cells/mL and exposed to different treatments. After adherence, cells were treated with the highest non-cytotoxic concentration of diferent extracts for 24h. A single reagent was added directly to cell culture treatments, generating cell lysis and luminescent signal proportional to the amount of ATP present in samples.

2.7. FOX01 expression through Western Blot and Indirect Immunofluorescence Assay

In order to evaluate the expression of FOX01 through western blot, HepG2 and HepG2/IRM cells were plated in 6-well plates at 3,0 x 10^5 cells/mL and exposed to different treatments for 24h. For the isolation of total protein fractions, the cells were collected, washed twice with ice-cold PBS, and lysed using cell lysis buffer (NP40, 20 mM Tris pH 7.5, 150 mM NaCl, 1% Triton X-100, 2.5 mM sodium pyrophosphate, 1 mM EDTA, protease inhibitor). The lysates were collected by scraping from the plates and then centrifuged at 14000 rpm at 4 °C for 5 min. Total protein was measured by taken 10μL of each sample and using a fluorometer system (Q33216 Qubit, Invitrogen), and equal quantity of samples were loaded on a 12% of SDS polyacrylamide gel electrophoresis and transferred onto polyvinylidene fluoride (PVDF) membrane (Millipore, Billerica, MA, USA) for 1 h. Membranes were

 doi:10.20944/preprints202308.0046.v1

blocked at room temperature for 1 h with blocking solution (5% power milk in TBST). After blocking, primary monoclonal antibody FOX01 (MA5-17078, Invitrogen) was incubated at 1:1000 overnight at 4°C, followed by incubation of secondary anti-mouse IgG (A5278, Sigma-Aldrich) for 1h at room temperature. For internal control, primary anti-human actin mouse Ab (1:1000 dilution, Cell Signaling) was used. After washing, the membranes were incubated for 1 h at room temperature with horseradish peroxidase (HRP)-linked anti-mouse IgG and immunoblots were performed using ECL prime WB detection kit (Amersham). Chemiluminescence visualization and detection was performed using ImageQuant LAS 500 (GE Healthcare life sciences).

For indirect immunofluorescence assay, cells were seeded into 6-well plates at 3,0 x 10^5 cells/mL. After 24 h incubation, cells were treated with different compounds for 24h, fixed with 2,5% glutaraldehyde for 20 min, permeabilized with 0,1% triton X for 15 min, blocked with 3% BSA for 30min, and incubated with the primary monoclonal anti-FOX01 antibody with 5µg/mL (MA5-17078, Invitrogen) for 1h at room temperature, followed by incubation with secondary anti-mouse fluorescein isothiocyanate (Anti-mouse IgG, Sigma, 1:150 v/v) for 1h. The slides mounted with coverslip and analyzed with a fluorescence light microscope (BX43 – Olympus).

2.8. Statistical Analysis

The results were expressed as mean ± standard deviation (SD) of three independent experiments performed in triplicate, used to assess normal distribution data. One-way analysis of variance (ANOVA) was applied, followed by Tukey post-hoc test. Statistically significant of mean differences was accepted at a level of $p \leq 0.05$.

3. Results and Discussion

3.1. Synthesis of Hydroxyhydroquinone

^{1}H and ^{13}C RMN and HRMS spectra of hydroxyhydroquinone is found in the supplementary material in Figure S1, S2 and S3. The product was stored under inert atmosphere (N_2) in dark conditions at room temperature to reduce hydroxy benzoquinone (HBQ) formation by air contact. ^{1}HNMR (D_2O, 300.18 MHz): δ (ppm) 6.21 (dd, 1H, J1=8.7 Hz, J2=3.0 Hz); 6.37 (d, 1H, J=3.7 Hz); 6.67 (d, 1H, J=8.4 Hz); ^{13}CNMR (D_2O, 75.49 MHz): 103.68 (CH), 106.62 (CH), 116.78 (CH), 137.14 (COH), 144.70 (COH), 149.26 (COH); HRMS negative ions: m/z, relative intensity (%): 123.0084, 10.9%, ($C_6H_3O_3$), [HBQ-H]$^-$, error 2.9 ppm; 125.0250, 100%, ($C_6H_5O_6$), [M-H]$^-$, error 4.9 ppm; 167.0365, 9.2%, ($C_8H_7O^4$), [M+CH_3CO-H]$^-$, error 9.1 ppm; 247.0263, 10.8%, ($C_{12}H_7O_6$), [2HBQ-H]$^-$, error 3.0 ppm; 249.0409, 21% ($C_{12}H_9O_6$), [M+HBQ-H]$^-$, error 1.9 ppm; 499. 0936, 3.9% ($C_{24}H_{19}O_{12}$), [2HHQ+2HBQ-H]$^-$, error 10.9 ppm. ^{1}H and ^{13}C NMR spectra confirms the data obtained by Humbarger et al. (2018) [14]. HRMS data show HBQ formation (oxidized form) as well as stable forms of clusters containing HHQ and HBQ formed in spectrometer source environment, once this compound aren't present in the NMR spectra. This characteristic of the hydroquinone-benzoquinone redox pair is known as quinhydrone.

3.2. P. crenata extract characterization

The results obtained by LCMS analysis (Table 1 and Figure 2) highlight that hydro-ethanolic extracts of *P. crenata* has quassinoids as major chemical class with 12 compounds and 87.5% of integrated area. The minor percentual areas are compound by furocoumarins (6.12%), β-carboline alkaloids (6.10%) and one flavonoid (0.23%). Results corroborate with Cardoso et al. (2009) [15].

Table 1. Chromatographic and chemical characterization data of stem hydro ethanolic extract of *P. crenata*.

Peak (min)	Experimental	Theoretical Mass	Error (ppm)	Compound
2.6	219.0250	219.0288	17.35	Dihydroxy furocoumarin

2.6	203.0504	203.0339	81.27	Hydroxy furocoumarin
2.7	381.0775	381.0816	10.76	Dihydroxy furocoumarin glycoside
8.7	268.0991	268.1179	70.12	(6,7-Dimethoxy-4-coumaryl) alanine
10.9	377.0805	377.0867	16.44	Limocitrol
13.1	365.1899	365.1959	16.43	Amarolide
13.8	393.1879	393.1908	7.37	6-hydroxy picrasin B
14.9	377.1932	377.1959	7.16	Picrasin B
15.7	393.1878	393.1908	7.63	Picraqualide C
16.3	435.1976	435.2013	8.5	Picraqualide D
16.6	241.0935	241.0972	15.34	Picrasidine 1
18.6	379.2090	379.2115	6.59	Nigakilactone A
19.0	379.2090	379.2115	6.59	Iso Nigakilactone A
19.5	389.1932	389.1959	6.94	Quassin
20.0	437.2120	437.2170	11.43	Picraqualide A
20.9	437.2121	437.2170	11.21	Iso Picraqualide A
22.5	387.1038	387.1074	9.30	Cleomiscosin A
23.1	340.1597	340.1543	15.87	Clausamine E
25.1	377.1878	377.1959	21.47	Parain
25.4	413.1892	413.1935	10.4	Neoquassin

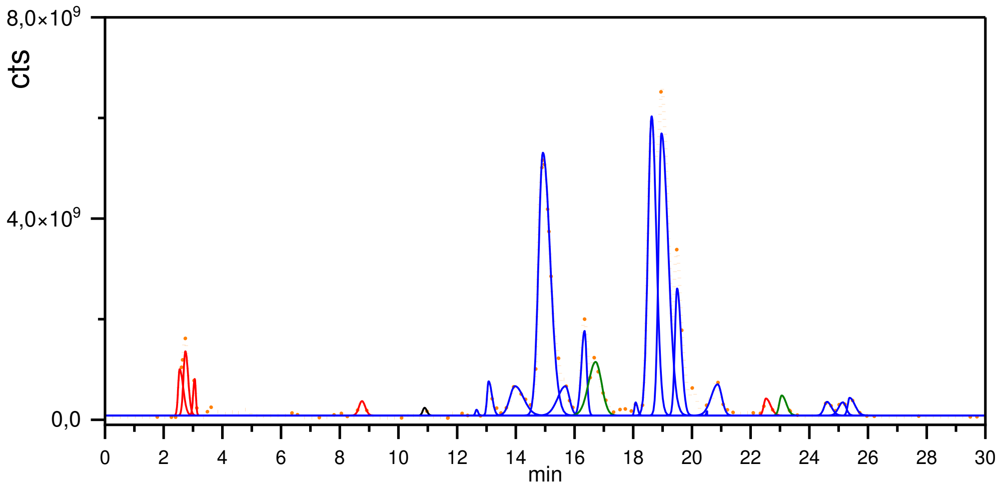

Figure 2. Extracted chromatograms of quassia extract analysis by LC-MS. Furocoumarins are highlighted in red, flavonoid in black, β-carboline alkaloids in green, quassinoids in blue and integral base peak chromatogram in dash orange.

Among the quassinoids identified in the *P. crenata* extract, the major compounds are picrasin B (22.5%), nigakilactone A (18.3%), iso nigakilactone A (19.7%), and quassin (5.6%), comprising 66% of the total chromatographic area. The data show that the *P. crenata* has a selective metabolic route for the biosynthesis of quassinoids, as well as a large storage capacity for these compounds in the woody part of the stem and branches. Our method proved to be robust and capable of detecting a series of quassinoids, β-carboline alkaloids and furocoumarins in the same analysis. Cardoso et al. (2009) [15] were able to determine parain α-dihydro-norneoquassin, quassin and a mixture of α-neoquassin and β-neoquassin using authentic standards with UV-Vis detection.

Lower concentration constituents, such as furocoumarins and β-carboline alkaloids are not mentioned in the literature for *P. crenata*. Zhao et al. (2016) [18] describes the identification of these classes of compounds isolated from *P. quassinoids* obtained in China. Along with quassinoids, β-carboline alkaloids and furocoumarins can be considered as chemical markers of plants of the genus *Picrasma*.

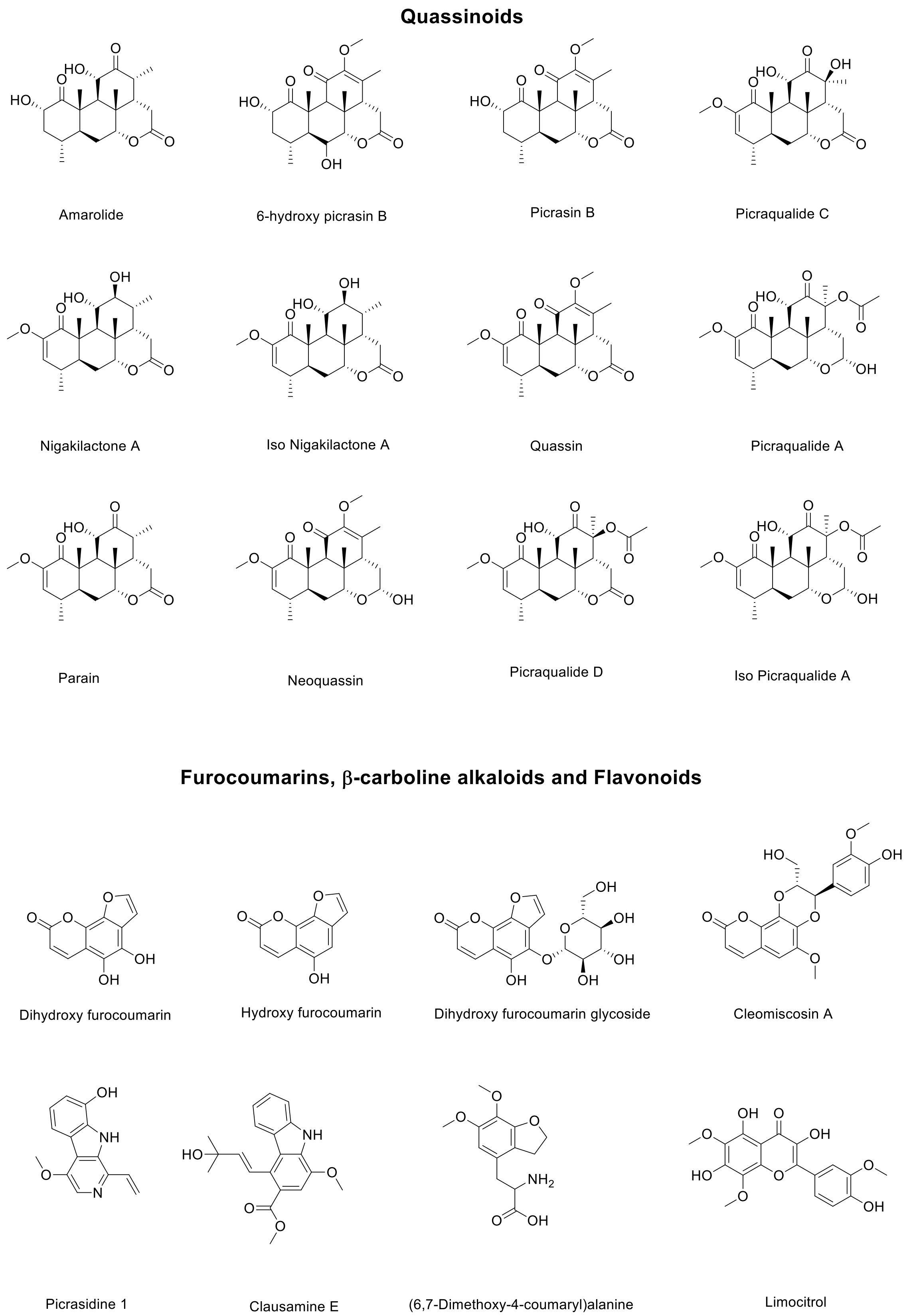

Figure 3. Chemical compounds detected in P. crenata extract by HPLC-ESI-MS.

3.3. R. cuspidata extract characterization

Rourea cuspidata extract was analyzed by ESI-TOF-MS by direct infusion in mode positive ions (Figure 4).

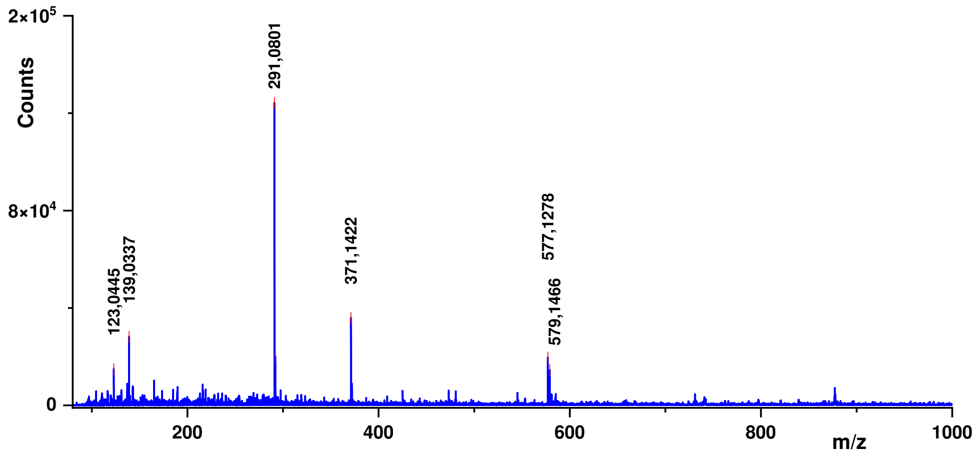

Figure 4. ESI-TOF-MS spectrum of R. cuspidate for positive ions.

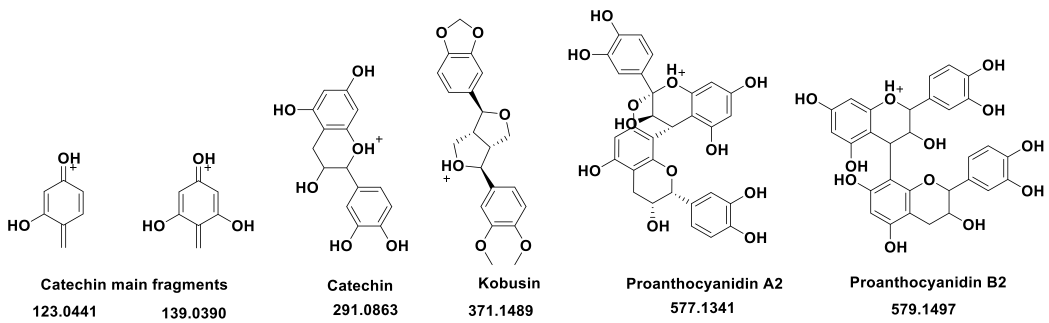

Figure 5. Main compounds obtained from ESI-TOF-MS analysis of *R. cuspidata*.

According to Laskowski et al. (2017) [10], mass spectrum has shown only polyphenolic compounds as proton adduct ions $[M+H]^+$ (Figure 5). Catechin are presented as the base peak (m/z 291.0801, error 3.9 ppm) with two minor fragments in m/z 123.0445 (error 10.5 ppm) and m/z 139.0337 (error 2.3 ppm). Kobusin was detected in m/z 371.1422 (error 0.6 ppm)and two proanthocyanidins (A2 and B2) were detected in m/z 577.1278 (error 1.0 ppm) and 579.1466 (error 2.7 ppm). According to Paim et al. (2022) [19], catechin, quercetin and proanthocyanidins comprise the highest concentration of phenolic compounds in plants of the genus Connaraceae, to which the pharmacological properties of these plants for the treatment of diseases associated with oxidative stress, such as type II diabetes, are attributed. According to Hussain et al. (2020) [8], Diabetes mellitus type 2 is a type of metabolic disorder. It develops due to the overproduction of free radicals, which results in increased oxidative stress. Some known damages of oxidative stress are defective insulin signals, glucose oxidation, and degradation of glycated proteins as well as alteration in glutathione metabolism, which induces hyperglycemia. Oxidative stress can be modulated by flavonoid ingestion.

3.4. Cell culture and cytotoxic assay

Hepatoma-derived cell lines show specific hepatocyte morphological characteristics and express hepatocyte-specific markers HepG2 cell line has been explored extensively for in vitro investigations on diabetes and insulin resistance [20]

The cytotoxic activity of all compounds was first monitored by MTT assay and compared to the control group without treatment through HepG2 and HepG2/IRM cell lines. A selection of the highest non-cytotoxic concentration of diferent extracts was obtained before establishing an insulin resistance model.

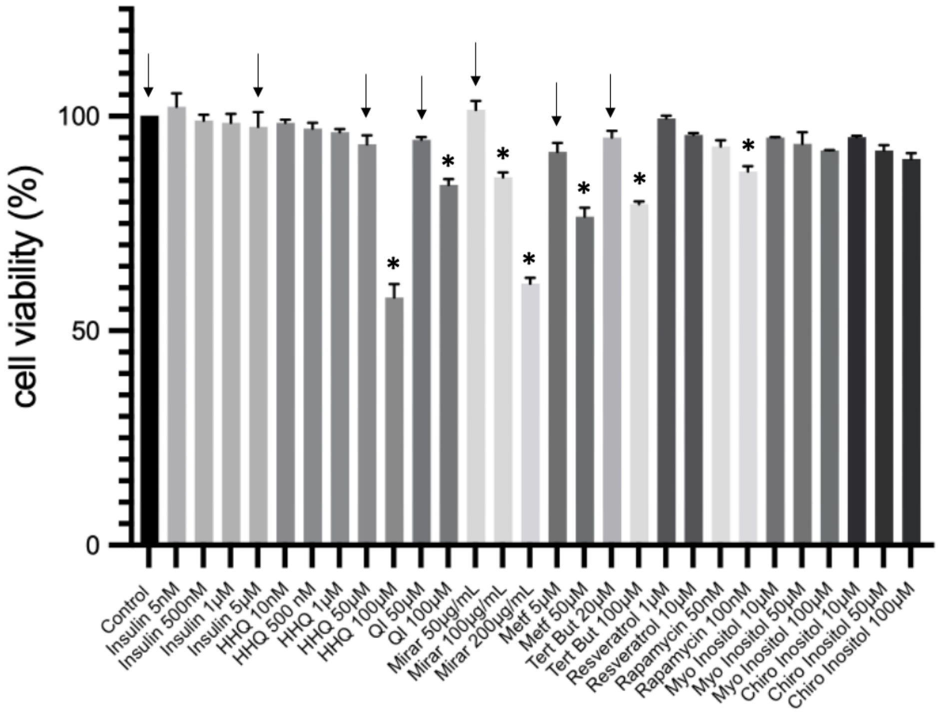

Figure 6. MTT assay: activity of isolated compounds and extracts against HepG2 cell line incubated for 24h. A selection of the highest non-cytotoxic concentration of diferent extracts was performed. Arrows are pointing the selection of compounds used for further experiments. The data were presented as mean ± SD (n = 3). One-way analysis of variance (ANOVA) test was used for multiple comparisons. *P ≤ 0.05 vs. control group.

A selection of compounds to be tested in further experiments was made upon MTT results, considering the highest non cytotoxic concentration. Arrows at figure 6 are pointing the selected molecules and concentrations, as following: insulin (INS -5µM); hydroxyhydroquinone (HHQ - 50 µM); isolated compounds from quassia extract (QI - 50 µM); miraruira extract (Mirar - 50 µg/mL); metformin (Met - 5µM); Tert-Butyl hydroperoxide - t-BHP (Tert But - 20 µM).

The hydroxyhydroquinone was synthetized as presented in section 2.1, and together with the quassinoids compounds (shown in section 2.2) are the main focus of this study. Miraruira is a popular name of *R. cuspidata Benth* ex. Baker, is a shrub of the Connaraceae family, common in Amazon region of Brazil, is used for diabetes treatment in folk medicine. The hypoglycemic activity of miraruira stem extracts has been explored in normal and streptozotocin-induced diabetic rats [10]. Metformin was selected as positive control compound, which has been used as medication for type 2 diabetes mellitus (T2DM) in the last decades. Research suggests that metformin stimulates peripheral glucose uptake while reducing hepatic glucose production [21] and attenuates triglyceride accumulation in HepG2 cells [22].

Other molecules explored in literature were also tested through MTT, such as resveratrol (Resv - 10 µM), rapamycin (Rapa - 100nM), Myo inositol and Chiro inositol (Myo Ino and Chiro Ino – 100 µM). Resveratrol is known as an active polyphenol and its effects have mainly been shown to be triggered due to its ability to activate AMP-activated protein kinase and sirtuin 1 in peripheral tissues of diabetic subjects [7]. Rapamycin plays an important role in insulin resistance model as an inhibitor of the mTOR regulation pathway [23]. Two types of inositol were also tested in this study once they are reported to promote glucose intake in high glucose environment. Chiro inositol (especially D-chiro) enhanced glucose consumption in high glucose-stimulating cells and increased the expression of insulin receptor substrate 2 (IRS2) protein in HepG2 cells [24].

3.5. Insulin resistance model (HepG2/IRM) and glucose uptake

Administration of inducers that can disrupt the insulin signaling pathway triggers insulin resistance in HepG2 cells. High glucose concentrations are known to induce cellular damage leading to glucose toxicity. Ultimately, high glucose concentrations lead to insulin resistance [20]. The exposure to high glucose triggers glucose production while suppressing glucose uptake in HepG2 [25]. High glucose levels interact with proteins and trigger the formation of excessive advanced glycation end products, which enhance oxidative stress. These conditions are prone to establish a phenotype of glucose toxicity, ROS accumulation, oxidative stress, and cell dysfunction, which trigger the progression of insulin resistance [26].

Before measuring glucose in media, a gradient of insulin at different concentrations (5nM – 5µM) was initially tested for viability through MTT. Insulin range corroborate with published data [7]. The highest non cytotoxic concentrations is represented in figure 6, and insulin at 5µM was selected according to the lower glucose consumption (data not shown). A selection of compounds (HHQ 50µM; QI 50µM; Mirar 50µg/mL; Metf 5µM, Tert But 20µM) was made according to non-cytotoxic parameters to be tested. The viability of insulin-resistance HepG2 cells was examined in the presence of different concentrations of compounds through MTT (Figure 7).

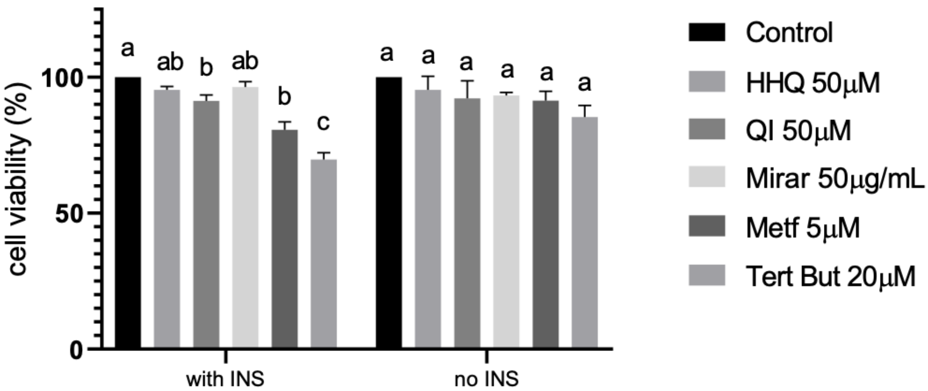

Figure 7. MTT assay: activity of isolated compounds and extracts against HepG2 and HepG2/IRM cell line incubated for 24h. A selection of the highest non-cytotoxic concentration of diferent extracts was performed. The data were presented as mean ± SD (n = 3). One-way analysis of variance (ANOVA) test was used for multiple comparisons, followed by Tukey. $P \leq 0.05$ - letters represent difference between groups.

Glucose concentration was determined using the glucose oxidase method through glucometer measurements. After 24h exposition to insulin at 5µM, cells were treated with the highest non-cytotoxic concentration of diferent extracts for 24h and glucose was measured after 24h of compounds incubation (Figure 8). All experiments were made in at least 3 replicates. The supernatant of the cells incubated with 5 µM of insulin showed the highest concentration of glucose left in media compared to control without insulin. The amount of glucose uptake in cells treated with insulin and further exposed to extracts of HHQ 50µM (5,68 ± 0,60 mmol/L) showed significant statistical levels compared to the remaining groups (Figure 8).

Preprints (www.preprints.org) | NOT PEER-REVIEWED | Posted: 2 August 2023 doi:10.20944/preprints202308.0046.v1

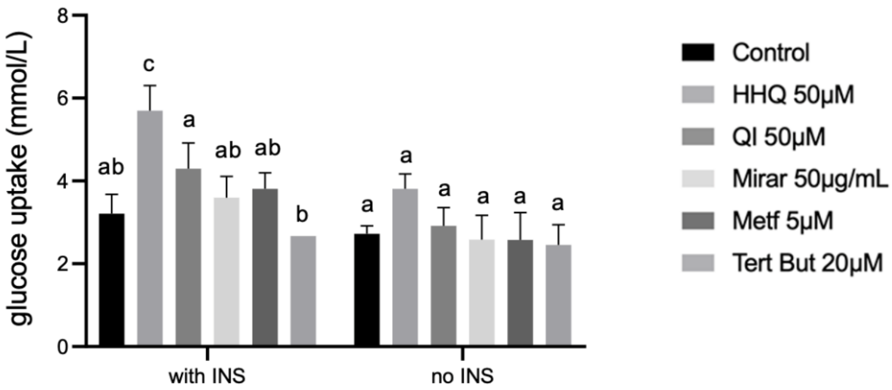

Figure 8. Glucose uptake concentration after treatment of HepG2/IRM cells with diferent extracts exposed to 24h compared to untreated HepG2/IRM cells. A decrease of glucose levels in medium (mmol/L) reflected in statistically significant increase of glucose uptake in cells with 5µM of insulin in sample exposed to 50µM of HHQ. *One-way analysis of variance (ANOVA) test was used for multiple comparisons, followed by Tukey. P ≤ 0.05 letters represent difference between groups.*

Tert-Butyl hydroperoxide (t-BHP) was applied as a pro-oxidant in the positive control group (tert but– 20µM) and presented statistical difference in the HepG2/IRM model. t-BHP is known to induce oxidative stress and cell injury that result from the intracellular increase production of ROS, data confirmed by flow cytometry in this study (Figure 9). t-BHP has been used in hepatocyte cultures and liver tissues, and its activity is metabolized to free radical intermediates, resulting in initiating lipid peroxidation, decreasing mitochondrial membrane potential, changes in mitochondrial membrane integrity [27]. Free radical intermediates generated by t-BHP can subsequently lead to oxidative-induced hepatocyte damage. Therefore, t-BHP has often been used to cause oxidative stress injury to in vitro cells, in order to identify antioxidant molecules from natural products [28].

3.6. ROS activity, Mitochondria Membrane Potential Assay and ATP balance

Oxidative stress has been recently recognized as a key mechanism in insulin resistance and is defined by excess endogenous oxidative species. ROS damage has direct roles in the development and progression of many chronic diseases, including the pathogenesis of insulin resistance and type 2 diabetes [29] t-BHP was able to induce oxidative stress and significantly increase production of ROS in both HepG2 and HepG2/IRM groups (Figure 9). As expected, ROS levels were increased in all treatments after insulin exposure. Most importantly, in the HepG2/IRM model, the cells that were exposed to HHQ (50 µM) and QI (50 µM) showed statistical difference of ROS levels compared to control.

Preprints (www.preprints.org) | NOT PEER-REVIEWED | Posted: 2 August 2023 doi:10.20944/preprints202308.0046.v1

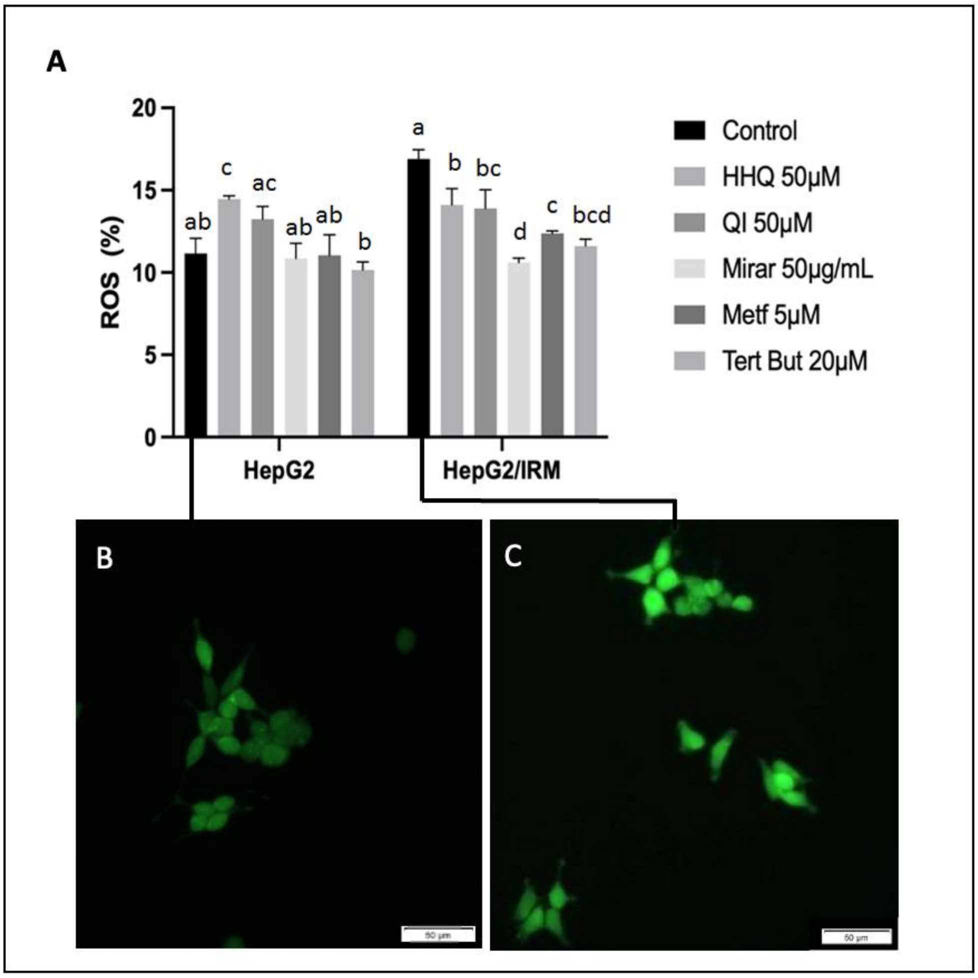

Figure 9. Effects of treatments of ROS levels on HepG2 and HepG2/IRM cells. A- Cells were analyzed by flow cytometry using the redox-sensitive fluorescent dye DCFH-DA as a marker of ROS production. Note that insulin resistant cell model (HepG2/IRM) increased ROS levels in all analyzed conditions compared to HepG2 without insulin induction. Images of DCFH-DA fluorescence on HepG2 (B) and HepG2/IRM (C) control groups. The data were presented as mean ± SD (n = 2). *One-way analysis of variance (ANOVA) test was used for multiple comparisons, followed by Tukey. P ≤ 0.05 letters represent difference between groups.*

Redox state of cells is crucial in health and disease equilibrium and opens redox-based prevention and therapeutic procedures in metabolic diseases such as inflammatory syndromes, obesity, aging, cardiovascular disease, metabolic syndrome, and diabetes [1,3,30,31]. In this context, cells treated with insulin and further exposed to HHQ (50 µM) and QI (50 µM) were the groups that showed higher amount of glucose uptake in cells (Figure 8), and maintained ROS levels lower than the ones observed in the control group (Figure 9). Mitochondria are one of the main sources of ROS and the major site of ATP production. When levels of glucose are high, mitochondria enhance ROS production and induce oxidative stress and tissue damage as a result [32]. Despite the existence of a variety of ROS origins such nitric oxide synthase, cytochrome p450, xanthine oxidase (XO), endoplasmic reticulum, peroxidases, and cyclooxygenases mitochondria and NADPH oxidases (NOX) are listed as major sites for ROS production [3].

The assessment of mitochondrial membrane potential in cells can yield information necessary for the evaluation of their physio-pathological conditions. Type 2 diabetes has been characterized by mitochondrial dysfunction, high production of reactive oxygen species (ROS) and low levels of ATP

Preprints (www.preprints.org) | NOT PEER-REVIEWED | Posted: 2 August 2023 doi:10.20944/preprints202308.0046.v1

[33]. The loss of mitochondrial membrane potential often takes place during the imbalance of cell signaling and induction of several disease [34].

HepG2 cell line and HepG2/IRM were treated with positive control t-BHP 20μM, which showed the highest depolarization rate in mitochondria, compared to other extracts like Mirar 50μg/mL, HHQ 50μM, QI 50 μM, Metf 5 μM. HepG2 and HepG2/IRM cells were stained with DiOC6 dye and change of fluorescent intensity was assessed by flow cytometry and statistically significant values were observed after treatment. Cells were also stained with a cationic dye JC-10 used in the mitochondria membrane potential assay. JC-10 is predominately localized in mitochondria and represents a fluorescent probe for the mitochondrial ΔΨ. This dye exhibits fluorescence emission at two wavelengths and Figure 10 show cells excited at 488 nm, green fluorescent J-monomers, indicating lost membrane potential after insulin exposition.

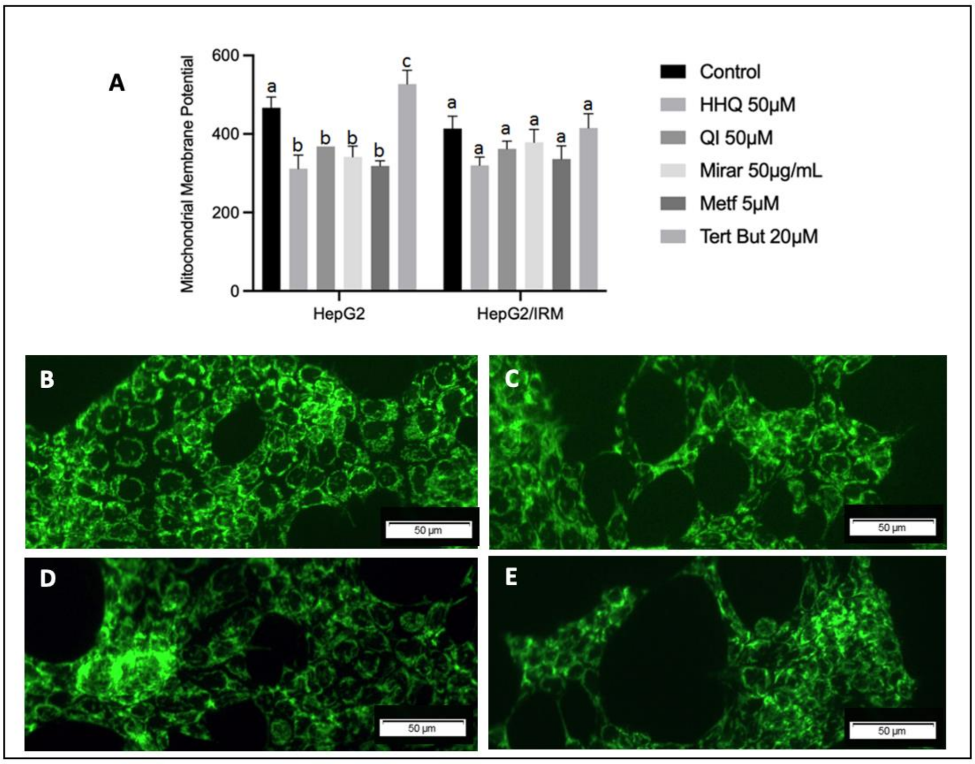

Figure 10. Mitochondria Membrane Potential assay with JC-10 dye against HepG2 cell line (A,B) and HepG2/IRM (C,D). A ,C– control samples; C,D – cells treated with t-BHP 100μM. Note that insulin resistant cell model present higher depolarization pattern in both control and t-BHP treated cells (HepG2/IRM) compared to HepG2 without insulin induction. One-way analysis of variance (ANOVA) test was used for multiple comparisons, followed by Tukey. P ≤ 0.05 letters represent difference between groups.

Mitochondrial membrane potential is generated as protons are pumped outward from the matrix, a process that depends on substrate utilization and electron transport. Loss of MMP will result from any process wherein protons move back toward the matrix generating nonspecific proton leaks and interactions with drug or chemical action [6]. In this process, HHQ and other phenolic compounds can act as ubiquinol and help transport electrons in the respiratory chain by the HHQ-HBQ redox pair in the mitochondrial membrane.

Insulin-resistant condition represent a higher risk of developing type 2 diabetes mellitus (T2DM) and cardiovascular disease compared with subjects which have normal insulin sensitivity. Literature points that metabolic regulation is largely dependent on mitochondria, which play an important role in energy homeostasis by metabolizing nutrients and producing ATP and heat [6]. According to our data, it is possible to observe that ATP values decreased in the insulin resistance model. Importantly,

Preprints (www.preprints.org) | NOT PEER-REVIEWED | Posted: 2 August 2023 doi:10.20944/preprints202308.0046.v1

once again the cells that were exposed to HHQ (50 μM) and QI (50 μM) in the HepG2/IRM model were grouped together with the control, showing no tendency of decrease in ATP levels (Figure 11).

Clinical evidence indicates that defects in mitochondrial function may be a primary cause of insulin resistance. Hence it is difficult clearly to ascertain whether defects in mitochondria occur before or after the onset of insulin resistance [6].

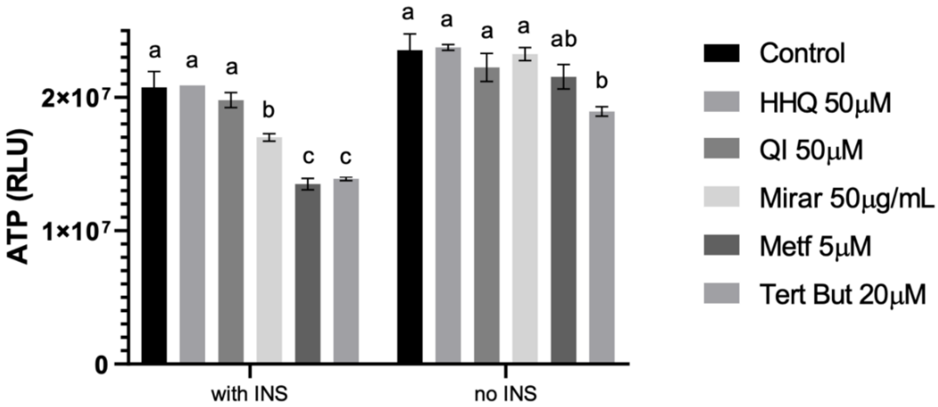

Figure 11. Effects of different compounds on adenosine triphosphate (ATP) levels using Luminescent system after 24h treatment, results given in relative light units (RLU). One-way analysis of variance (ANOVA) test was used for multiple comparisons, followed by Tukey. $P \leq 0.05$ letters represent difference between groups.

Glucose and lipid metabolism are largely dependent on mitochondria to generate energy in cells. Thereby, when nutrient oxidation is inefficient, the ratio of ATP production/oxygen consumption is low, leading to an increased production of superoxide anions [5]. Our results showed a decrease in ATP on HepG2/IRM treated with metformin (5μM), which may indicate that the extra availability of glucose promoted by metformin can induce less profitable ATP pathways (Figure 11). A possible pathway is promoting anaerobic glycolysis instead of cellular respiration, which explains the reduction in ATP production by the mitochondria. According to Zang et al. (2004) [35] there is biochemical evidence that the effects of metformin on the lipid content of HepG2 cells depend on activation of AMPK, being the principal mediator of the effects of metformin on lipid biosynthesis, and elevating lipids associated with insulin-resistant state. These statements also corroborate with a study from Dykens et al. (2008) [36], that HepG2 cells accelerate glycolytic flux in a compensatory way, which correspondingly increases lactate efflux. This mechanism requires tissue glucose uptake, so that the desired clinical goal for these drugs of reducing hyperglycemia is achieved.

Molecular and cellular mechanisms of insulin resistance are relevant to understanding the pathogenesis of various diseases. Insulin resistance is characterized by a diminished ability of cells or tissues to respond to physiological levels of insulin [5]. Impaired insulin signaling not only affects insulin-stimulated glucose metabolism in skeletal muscle, but also damages other insulin regulation in diverse tissues including liver, the in vitro model used in this study [5].

It has been stated that diabetes and mitochondrial function in non–insulin-sensitive tissues present a glucose uptake metabolism independent of circulating insulin, but highly affected by the blood glucose concentration [5]. Hyperglycemia in these insulin-independent tissues appears to generate increased mitochondrial substrates and increase the propensity for ROS production.

3.7. FOX01 expression through Western Blot and Indirect Immunofluorescence Assay

Forkhead box class O (FoxO) proteins are nuclear transcription factors that participate in the regulation of various cellular processes [37] Are reported as major intracellular targets of insulin action and contribute to the regulation of gluconeogenic, glycolytic gene expression and nutrient

Preprints (www.preprints.org) | NOT PEER-REVIEWED | Posted: 2 August 2023 doi:10.20944/preprints202308.0046.v1

metabolism in the liver [38,39]. One of its members, FoxO1, has been shown to interact directly with DNA binding sites involved in gluconeogenesis and promote glucose production, both in isolated hepatocytes [40] and in transgenic mouse models [39].

FoxO1 has its activity suppressed by insulin, which could be seen in control group from the experiments conducted in this study through western blot and immunofluorescence (Figure 12). After insulin incubation and exposure to different treatments, FOX01 expression significantly decreased in cell treated with hydroxyhydroquinone (HHQ 50 μM), and cells exposed to quassinoid (QI 50 μM) compounds maintained lower expression compared to cells without insulin treatment. Cells treated with miraruira extract (Mirar 50 μg/mL) maintained high levels of FoxO1, despite presenting promising levels of glucose cell uptake (Figure 8) and the lowest levels of ROS from all compounds tested after insulin cell exposure (Figure 9).

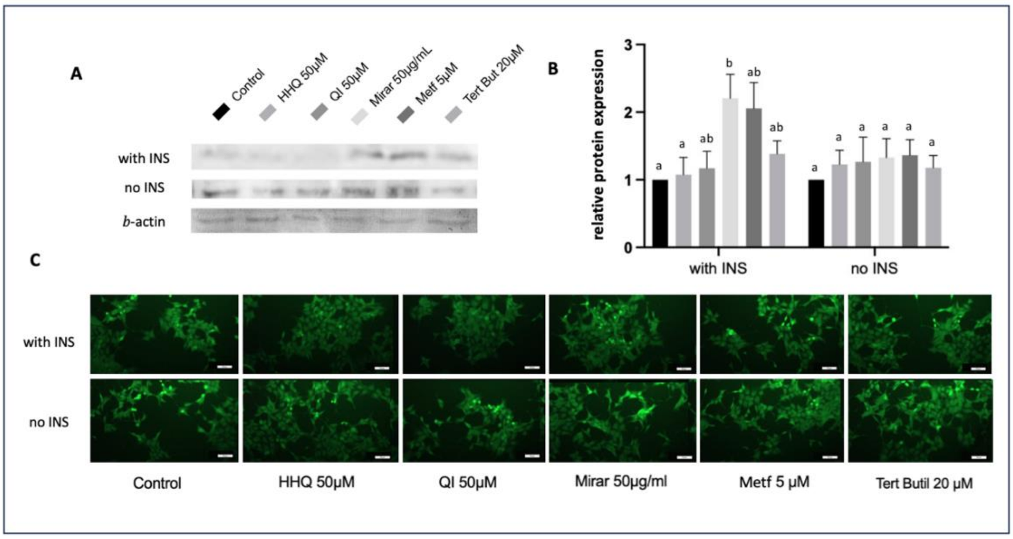

Figure 12. FOX01 expression through western blot and indirect immunofluorescence assay in HepG2 and HepG2/IRM cells. A) Western blot analysis of FoxO1 and b-actine; B) Densitometric analysis of western blot normalized to b -actin of control using ImageJ; C) Indirect immunofluorescence using anti-FoxO1. One-way analysis of variance (ANOVA) test was used for multiple comparisons, followed by Tukey. $P \leq 0.05$ letters represent difference between groups.

Once insulin is presented to cells, it binds to the insulin receptor (IR), activates Akt and phosphorylates FoxO1 proteins, resulting in their translocation from the nucleus to the cytoplasmic compartment [41]. Recent studies have pointed that insulin/PI3K/Akt signaling pathway is activated through insulin uptake in cells, this mechanism stimulates glycogen synthesis and inhibits gluconeogenesis in the liver, leading to a reduction in plasma glucose levels [42]. This demonstrates that hepatocytes play a crucial role in the pathogenesis of insulin resistance. Consequently, the HepG2 cell line could provide a valuable tool for identifying drug candidates that target the insulin/PI3K/Akt pathway in the liver [20].

Glucose restoration after suppression of FoxO1 in HepG2/IRM models has also been reported through in vitro studies, which corroborates with our findings [13,43–45]. In fact, the group of cells treated with hydroxyhydroquinone and quassinoid compounds were the ones that decreased FoxO1 expression and presented higher levels of glucose cell uptake after treatments (Figure 8). Furthermore, flow cytometry analysis revealed that regular levels of ROS and MMP were maintained for these two groups of compounds in HepG2/IRM model (Figure 9 and 10). In an interesting way, the same compounds, HHQ and QI, were able to retain ATP levels comparable to the control after insulin exposure (Figure 11). In fact, the reduction of FoxO1 expression by the cell treated with quassinoids (QI) seems to occur by the inhibition of the cortisol nuclear receptor, since the compound activates the FoxO1 expression cascade to direct the metabolism towards gluconeogenesis.

It is stated that insulin-mediated suppression of liver FoxO1 activity plays a critical role in glucose homeostasis and is crucial for inhibition of hepatic glucose production by insulin [12]. Literature has also pointed out through in vivo studies that disruption of FoxO1 restores glucose tolerance in mice [46,47] and that FoxO1 inhibition may even reactivate the ability of insulin to suppress hepatic glucose production in mice in which Akt signaling has been disrupted [15]. This finding has suggested that FoxO1 not only mediates metabolic consequences of liver insulin resistance, but also that hepatic glucose metabolism can be controlled via other insulin signaling pathways when the activity of FoxO1 has been disrupted [48].

Given its complexity, FoxO1 expression may be regulated under several conditions. In the liver of mice after chronic stress, FoxO1 levels are shown to be increased and involved in the lipid metabolism. The expression of FOXO1 is also activated by cortisol and its binding to the nuclear glucocorticoid receptor, which is the main mechanism of induction of insulin resistance initiated by stress [49]. Therefore, steroidal compounds with glucocorticoid action such as quassinoids presented in this study, can act by competing with the nuclear glucocorticoid receptor and to inhibit the production of FOXO1 and induce cellular sensitivity to insulin. These findings offer a novel mechanistic understanding of the beneficial effects of hydroxyhydroquinone and quassinoids on hepatic insulin resistance, to assist in the treatment of insulin resistance and diabetes in the future.

4. Conclusions

The findings presented in this work offer a novel understanding of the beneficial effects of hydroxyhydroquinone and quassinoids compounds against in vitro hepatic insulin resistance model. Hydroxyhydroquinone has been synthetized for applications unrelated to animal and human health and its effects in HepG2/IR model are extremely promising. Quassinoids also need special attention given its similarities to glucocorticoid activity, which can act by competing with the nuclear glucocorticoid receptor and to inhibit the production of FoxO1.

It is important to understand the mechanisms involved in the activation of FoxO1 and how its function affects the liver and the organism integrally. It is also crucial to track back FoxO1 for insulin-regulated signals elsewhere from the hepatic region, these may interfere in regulating hepatic glucose metabolism. Suppressing FoxO1 in the liver is stated to be required for extrahepatic effects of insulin to be effective in regulating hepatic glucose metabolism [12]. Therefore, in vivo studies with rodents are mandatory to continue investigating the molecular mechanisms underlying these promising compounds that may contribute to assist in the treatment of insulin resistance and diabetes in the future.

Supplementary Materials: The following supporting information can be downloaded at the website of this paper posted on Preprints.org, Figure S1: Figure S 1. HRMS spectrum for HHQ compound obtained by ESI-TOF-MS in mode negative ions. Figure S 2. ^{1}HNMR spectrum for HHQ obtained in D_2O at 300.18 MHz. Figure S 3. ^{13}CNMR spectrum for HHQ obtained in D_2O at 75.49 MHz.

Author Contributions: P. R. S. and S. D. carried out the gutting, processing and extraction of plant material from *P. crenata* and *R. cuspidata*, processed the chemical analysis and treatment of LCMS and HRMS data. P. R. S. carried out the synthesis, isolation and chemical characterization of the HHQ and helped with the writing of the text of the paper. M. R. E. coordinated and carried out all the biochemical experiments, processing, graph plotting, bibliographic search and writing of the paper. W.V.S, R.F and F.S. helped in the elaboration of the biochemical experiments and in the production and statistical of data. S. M. assisted in granting the material and providing laboratory instrumentation for chemical analyses. A. J. R. assisted in granting research material. All authors have read and agreed to submit the manuscript.

Funding: This research received no external funding.

Conflicts of Interest: The authors declare no conflict of interest.

References

1. Magnani, N.D.; Marchini, T.; Calabró, V.; Alvarez, S.; Evelson, P. Role of Mitochondria in the Redox Signaling Network and Its Outcomes in High Impact Inflammatory Syndromes. Front Endocrinol (Lausanne). **2020**, *11*, 568305. doi: 10.3389/fendo.2020.568305.

2. Holmström, K.; Finkel, T. Cellular mechanisms and physiological consequences of redox-dependent signalling. *Nat Rev Mol Cell Biol*. **2014**, *15*, 411-421. https://doi.org/10.1038/nrm3801
3. Cervantes, G. K.; Llanas-Cornejo, D.; Husi, H. CVD and Oxidative Stress. J Clin Med. **2017**, *6(2)*, 22. doi: 10.3390/jcm6020022.
4. Daiber, A.; Di Lisa, F.; Oelze, M.; Kröller-Schön, S.; Steven, S.; Schulz, E.; Münzel, T. Crosstalk of mitochondria with NADPH oxidase via reactive oxygen and nitrogen species signalling and its role for vascular function. Br J Pharmacol. **2017**, *174(12)*, 1670-1689. doi: 10.1111/bph.13403.
5. Kim, J.A.; Wei, Y.; Sowers, J.R. Role of mitochondrial dysfunction in insulin resistance. Circ Res. **2008**, *102(4)*, 401-14. doi: 10.1161/circresaha.107.165472.
6. Sivitz, W.I.; Yorek, M.A. Mitochondrial dysfunction in diabetes: from molecular mechanisms to functional significance and therapeutic opportunities. Antioxid Redox Signal. **2010,** *12(4)*, 537-77. doi: 10.1089/ars.2009.2531.
7. Teng, W.; Yin, W.; Zhao, L.; Ma, C.; Huang, J.; Ren, F. Resveratrol metabolites ameliorate insulin resistance in HepG2 hepatocytes by modulating IRS-1/AMPK. RSC Adv. **2018**, *8*, 36034–36042. Doi: 10.1039/c8ra05092a
8. Hussain, T.; Tan, B.; Murtaza, G.; Liu, G.; Rahu, N.; Kalhoro, M. S.; Kalhoro, D. H.; Adebowale, T.O.; Mazhar, M. U.; Rehman, Z.U.; Martínez, Y.; Khan, S.A.; Yin, Y. Flavonoids and type 2 diabetes: Evidence of efficacy in clinical and animal studies and delivery strategies to enhance their therapeutic efficacy. Pharmacol Res. **2020,** *152*, 104629. doi: 10.1016/j.phrs.2020.104629.
9. Kargl, C.; Arshad, M.; Salman, F.; Schurman, R.C.; Del Corral, P.. 11β-hydroxysteroid dehydrogenase type-II activity is affected by grapefruit juice and intense muscular work. Arch Endocrinol Metab. **2017**, *61*/*6*, 556-561. https://doi.org/10.1590/2359-3997000000296
10. Laikowski, M.M.; Santos, P.R.; Souza, D.M.; Minetto, L.; Girondi, N.; Pires, C.; Alano, G.; Roesch-Ely, M.; Tasso, L.; Moura, S. Rourea cuspidata: Chemical composition and hypoglycemic activity. Asian Pac J Trop Biomed. **2017**, *7(8)*, 712–718. https://doi.org/10.1016/j.apjtb.2017.07.015
11. Mauro, A.L.Q.S. Study of the hypoglicemic activity of the tea of the wood of Quassia-do-Brasil, Picrasma crenata (Vell.) Engl. in mice and rats. Vig Sanit Debate. **2015**, *3(1)*, 116-122.
12. 12-O-Sullivan, I.; Zhang, W.; Wasserman, D.; Liew, C.W.; Liu, J.; Paik, J.; DePinho, R.A.; Stolz, D.B.; Kahn, C.R.; Schwartz, M.W.; Unterman, T.G. FoxO1 integrates direct and indirect effects of insulin on hepatic glucose production and glucose utilization. Nat Commun. **2015**, *6*, 7079. https://doi.org/10.1038/ncomms8079
13. Zhang, H.; Ge, Z.; Tang, S.; Meng, R.; B,i Y.; Zhu, D. Erythropoietin ameliorates PA-induced insulin resistance through the IRS/AKT/FOXO1 and GSK-3β signaling pathway, and inhibits the inflammatory response in HepG2 cells. Mol Med Rep. **2017**, *16*, 2295-2301. https://doi.org/10.3892/mmr.2017.6810
14. Humbarger, Scott Thomas, and Millard, Matthew. 2018.United States Patent. US Patent 10,065,977 B2. Sep 4.
15. Cardoso, M. L. C.; Kamei, M.S.; Nunes, R.F.; Lazeri, N.S.; Neto, J.R.S.; Novello, C.R.; Bruschi, M.L. Development and Validation of an HPLC Method for Analysis of *Picrasma crenata*. Journal of Liquid Chromatography & Related Technologies. **2008**, *1*, *32*, 72–79. https://doi.org/10.1080/10826070802548663
16. Kheirollahzadeh, F.; Eftekhari, E.; Ghollasi, M.; Behzadi, P. Anti-hyperglycemic effects of Eryngium billardierei F. Delaroche extract on insulin-resistance HepG2 cells in vitro. Mol Bio Rep. **2022**, *49*, 3401–3411. https://doi.org/10.1007/s11033-022-07171-0
17. Frozza, C.O.D.S.; Santos, D.A.; Rufatto, L.C.; Minetto, L.; Scariot, F.J.; Echeverrigaray, S.; Pich, C.T.; Moura, S.; Padilha, F.F.; Borsuk, S.; Savegnago, L.; Collares, T.; Seixas, F.K.; Dellagostin, O.; Roesch-Ely, M.; Henriques, J.A.P. Antitumor activity of Brazilian red propolis fractions against Hep-2 cancer cell line. Biomed Pharmacother. **2017**, *91*, 951-963. doi: 10.1016/j.biopha.2017.05.027.
18. Zhao, S.; Kanno, Y.; Li, W.; Sasaki, T.; Zhang, X.; Wang, J.; Cheng, M.; Koike, K.; Nemoto, K.; Li, H. Identification of Picrasidine C as a Subtype-Selective PPARα Agonist. J Nat Prod. **2016**, *79(12)*, 3127-3133. doi: 10.1021/acs.jnatprod.6b00883.
19. Paim, L.F.N.A.; Santos, P.R.; Toledo, C.A.P.; Minello, L.; Paz, J.R.L.; Souza, V.C.; Salvador, M.; Moura, S. Four almost unexplored species of Brazilian Connarus (Connaraceae): Chemical composition by ESI-QTof-MS/MS-GNPS and a pharmacologic potential. Phytochem Anal. **2022**, *33(2)*, 286-302. doi: 10.1002/pca.3087.
20. Yudhani, R.D.; Sari, Y.; Nugrahaningsih, D.A.A.; Sholikhah, E.N.; Rochmanti, M.; Purba, A.K.R.; Khotimah, H.; Nugrahenny, D.; Mustofa, M. In Vitro Insulin Resistance Model: A Recent Update. Journal of Obesity. **2023**, 1-13. https://doi.org/10.1155/2023/1964732
21. Azimian, L.; Weerasuriya, N.M.; Munasinghe, R.; Song, S.; Lin, C.Y.; You, L. Investigating the effects of Ceylon cinnamon water extract on HepG2 cells for Type 2 diabetes therapy. Cell Biochem Funct. **2023**, *41*, 254–267.
22. Zhu, X.; Yan, H.; Xia, M.; Chang, X.; Xu, X.; Wang, L.; Sun, X.; Lu, Y.; Bian, H.; Li, X.; Gao, X. Metformin attenuates triglyceride accumulation in HepG2 cells through decreasing stearyl-coenzyme A desaturase 1 expression. Lipids in Health and Disease. **2018**, *17*, 114.

23. Jiang, H.; Ma, Y.; Yan, J.; Liu, J.; Li, L. Geniposide promotes autophagy to inhibit insulin resistance in HepG2 cells via P62/NF-κB/GLUT-4. Molecular Medicine Reports. **2017**, *16*, 7237-7244.
24. Fan, C.; Liang, W.; Wei, M.; Gou, X.; Han, S.; Bai, J. Effects of D-Chiro-Inositol on Glucose Metabolism in db/db Mice and the Associated Underlying Mechanisms. Frontiers in Pharmacology. **2020**, *11*, 354.
25. Zhu, Y.X.; Hu, H.Q.; Zuo, M.L.; Mao, L.; Song, G.L.; Li, T.M.; Dong, L.C.; Yang, Z.B.; Ali Sheikh, M.S. Effect of oxymatrine on liver gluconeogenesis is associated with the regulation of PEPCK and G6Pase expression and AKT phosphorylation. Biomed Rep. **2021**, *1*, 56. doi: 10.3892/br.2021.1432.
26. Giri, B.; Dey, S.; Das, T.; Sarkar, M.; Banerjee, J.; Dash, S.K. Chronic hyperglycemia mediated physiological alteration and metabolic distortion leads to organ dysfunction, infection, cancer progression and other pathophysiological consequences: An update on glucose toxicity. Biomed Pharmacother. **2018**, *107*, 306-328. doi: 10.1016/j.biopha.2018.07.157.
27. Tsai, T.H.; Yu, C.H.; Chang, Y.P.; Lin, Y.T.; Huang, C.J.; Kuo, Y.H.; Tsai, P.J. Protective Effect of Caffeic Acid Derivatives on tert-Butyl Hydroperoxide-Induced Oxidative Hepato-Toxicity and Mitochondrial Dysfunction in HepG2 Cells. Molecules. **2017**, *22(5)*, 702. doi: 10.3390/molecules22050702.
28. Park, C.L.; Kim, J.H.; Jeon, J.S.; Lee, J.H.; Zhang, K.; Guo, S.; Lee, D.H.; Gao, E.M.; Son, R.H.; Kim, Y.M.; Park, G.H.; Kim, C.Y. Protective Effect of *Alpinia oxyphylla* Fruit against *tert*-Butyl Hydroperoxide-Induced Toxicity in HepG2 Cells via Nrf2 Activation and Free Radical Scavenging and Its Active Molecules. Antioxidants (Basel). **2022**, *11(5)*, 1032. doi: 10.3390/antiox11051032.
29. Hurrle, S.; Hsu, W.H. The etiology of oxidative stress in insulin resistance. Biomed Journal. **2017**, *40(5)*, 257-262. doi: 10.1016/j.bj.2017.06.007
30. Almeida, C.; Monteiro, C.; Silvestre, S. Inhibitors of 11β-Hydroxysteroid Dehydrogenase Type 1 as Potential Drugs for Type 2 Diabetes Mellitus—A Systematic Review of Clinical and In Vivo Preclinical Studies. *Sci. Pharm.* **2021**, *89*, 5. https://doi.org/10.3390/scipharm89010005
31. Korac, B.; Kalezic, A.; Pekovic-Vaughan, V.; Korac, A.; Jankovic, A. Redox changes in obesity, metabolic syndrome, and diabetes. Redox Biol. **2021**, *42*, 101887. doi: 10.1016/j.redox.2021.101887.
32. Szendroedi, J.; Phielix, E.; Roden, M. The role of mitochondria in insulin resistance and type 2 diabetes mellitus. Nat Rev Endocrinol. **2011**, *8(2)*, 92-103. doi: 10.1038/nrendo.2011.138.
33. Rovira-Llopis, S.; Bañuls, C.; Diaz-Morales, N.; Hernandez-Mijares, A.; Rocha, M.; Victor, V.M. Mitochondrial dynamics in type 2 diabetes: Pathophysiological implications. Redox Biol. **2017**, *11*, 637-645. doi: 10.1016/j.redox.2017.01.013.
34. Elefantova, K.; Lakatos, B.; Kubickova, J.; Sulova, Z.; Breier, A. Detection of the Mitochondrial Membrane Potential by the Cationic Dye JC-1 in L1210 Cells with Massive Overexpression of the Plasma Membrane ABCB1Drug Transporter. Int J Mol Sci. **2018**, *19*, 1985. doi:10.3390/ijms19071985.
35. Zang, M.; Zuccollo, A.; Hou, X.; Nagata, D.; Walsh, K.; Herscovitz, H.; PBrecher, P.; Ruderman, N.B.; Cohen, R.A. AMP-activated Protein Kinase Is Required for the Lipid-lowering Effect of Metformin in Insulin-resistant Human HepG2 Cells. The J Biol Chem. **2004**, *279(46)*, 47898–47905. doi: 10.1074/jbc.M408149200.
36. Dykens, J.A.; Jamieson, J.; Marroquin, L.; Nadanaciva, S.; Billis, P.A.; Will, Y. Biguanide-induced mitochondrial dysfunction yields increased lactate production and cytotoxicity of aerobically-poised HepG2 cells and human hepatocytes in vitro. Toxicol Appl Pharmacol. **2008**, *233*, 203–210. doi: 10.1016/j.taap.2008.08.013.
37. Bielka, W.; Przezak, A. The role of FOXO transcription factors in the development of type 2 diabetes and related potential therapeutic possibilities. Clinical Diabetology. **2021**, *10 (3)*, 290-298. Doi: 10.5603/DK.a2021.0021
38. Zhang, W.; Patil, S.; Chauhan, B.; Guo, S.; Powell, D.R.; Le, J.; Klotsas, A.; Matika, R.; Xiao, X.; Franks, R.; Heidenreich, K.A.; Sajan, M.P.; Farese, R.V.; Stolz, D.B.; Tso, P.; Koo, S.H.; Montminy, M.; Unterman, T.G. FoxO1 regulates multiple metabolic pathways in the liver: effects on gluconeogenic, glycolytic, and lipogenic gene expression. J Biol Chem. **2006**, *281(15)*, 10105-17. doi: 10.1074/jbc.M600272200.
39. Zhang, K.; Li, L.; Qi, Y.; Zhu, X.; Gan, B.; DePinho, R.A.; Averitt, T.; Guo, S. Hepatic suppression of Foxo1 and Foxo3 causes hypoglycemia and hyperlipidemia in mice. Endocrinology. **2012**, *153(2)*, 631-46. doi: 10.1210/en.2011-1527.
40. Puigserver, P.; Rhee, J.; Donovan, J.; Walkey, C.J.; Yoon, J.C.; Oriente, F.; Kitamura, Y.; Altomonte, J.; Dong, H.; Accili, D.; Spiegelman, B.M. Insulin-regulated hepatic gluconeogenesis through FOXO1–PGC-1α interaction. Nature. **2003**, *423*, 550–555. https://doi.org/10.1038/nature01667
41. Brunet, A.; Bonni, A.; Zigmond, M.J.; Lin, M.Z.; Juo, P.; Hu, L.S.; Anderson, M.J.; Arden, K.C.; Blenis, J.; Greenberg, M.E. Akt promotes cell survival by phosphorylating and inhibiting a Forkhead transcription factor. Cell. **1999**, *96(6)*, 857-68. doi: 10.1016/s0092-8674(00)80595-4.
42. Dou, Z.; Liu, C.; Feng, X.; Xie, Y.; Yue, H.; Dong, J.; Zhao, Z.; Chen, G.; Yang, J. Camel whey protein (CWP) ameliorates liver injury in type 2 diabetes mellitus rats and insulin resistance (IR) in HepG2 cells via activation of the PI3K/Akt signaling pathway. Food Funct. **2022**, *13(1)*, 255-269. doi: 10.1039/d1fo01174j.
43. Zhang, Y.; Yan, L.S.; Ding, Y.; Cheng, B.C.Y.; Luo, G.; Kong, J.; Liu, T.H.; Zhang, S.F. *Edgeworthia gardneri* (Wall.) Meisn. Water Extract Ameliorates Palmitate Induced Insulin Resistance by Regulating

IRS1/GSK3β/FoxO1 Signaling Pathway in Human HepG2 Hepatocytes. *Front. Pharmacol.* **2020**, *10*, 1666. doi: 10.3389/fphar.2019.01666.

44. Chen, L.; Sun, X.; Xiao, H.; Xu, F.; Yang, Y.; Lin, Z.; Chen, Z.; Quan, S.; Huang, H. PAQR3 regulates phosphorylation of FoxO1 in insulin-resistant HepG2 cells via NF-κB signaling pathway. Exp Cell Res. **2019,** *381(2)*, 301-310. doi: 10.1016/j.yexcr.2019.04.031.
45. Rong Guo, X.; Li Wang, X.; Chen, Y.; Hong Yuan, Y.; Mei Chen, Y.; Ding, Y.; Fang, J.; Jiao Bian, L.; Sheng Li, D. ANGPTL8/betatrophin alleviates insulin resistance via the Akt-GSK3β or Akt-FoxO1 pathway in HepG2 cells. Exp Cell Res. **2016**, *345(2)*, 158-67. doi: 10.1016/j.yexcr.2015.09.012.
46. Dong, X.C.; Copps, K.D.; Guo, S.; Li, Y.; Kollipara, R.; DePinho, R.A.; White, M.F. Inactivation of hepatic Foxo1 by insulin signaling is required for adaptive nutrient homeostasis and endocrine growth regulation. Cell Metab. **2008**, *8(1)*, 65-76. doi: 10.1016/j.cmet.2008.06.006.
47. Lu, M.; Wan, M.; Leavens, K.F.; Chu, Q.; Monks, B.R.; Fernandez, S.; Ahima, R.S.; Ueki, K.; Kahn, C.R.; Birnbaum, M.J. Insulin regulates liver metabolism in vivo in the absence of hepatic Akt and Foxo1. Nat Med. **2012**, *18(3)*, 388-95. doi: 10.1038/nm.2686.
48. Cheng, Z.; White, M.F. The AKTion in non-canonical insulin signaling. Nat Med. **2012**, *18(3)*, 351-353. doi: 10.1038/nm.2694.
49. Liu, Y.Z.; Peng, W.; Chen, J.K.; Su, W.J.; Yan, W.J.; Wang, Y.X.; Jiang, C.L. FoxO1 is a critical regulator of hepatocyte lipid deposition in chronic stress mice. PeerJ. **2019**, *7*, 7668. doi: 10.7717/peerj.7668.